Check for updates

# Synthesis and characterization of novel star-branched polyimides derived from 2,2-bis[4-(2,4-diaminophenoxy)phenyl]hexafluoropropane

Feng Wu, Xingping Zhou [ID]* and Xinhai Yu [ID]*

A novel aromatic fluorinated tetramine, 2,2-bis[4-(2,4-diaminophenoxy)phenyl]hexafluoropropane (BDAPFP), was successfully synthesized. To maximize the advantages of the linear polyimides and hyperbranched polyimides, a series of novel star-branched fluorinated polyimides BPI-(1−3), which were derived from BDAPFP and anhydride-terminated linear poly(amide acid)s LPAA'-(1−3), were successfully synthesized. For comparison, a series of corresponding linear polyimides LPI-(1−3) were prepared from 4,4'-oxybisbenzenamine (ODA), *p*-phenylenediamine (PDA) and 3,3',4,4'-biphenyltetracarboxylic dianhydride (BPDA) with various monomer ratios *via* the conventional two-step procedure with heating, imidization method. All the polyimides could form strong, flexible and transparent films with an UV-visible absorption cut-off wavelength at 366−398 nm. When compared with the linear polyimide films LPI-(1−3), the star-branched fluorinated polyimide films BPI-(1−3) not only possessed better thermal stability with glass transition temperatures of 283.0−318.0 °C and 5% weight loss temperatures of 544−578 °C and 500−560 °C in nitrogen and air, respectively, but also had improved mechanical properties with tensile strengths of 113−243 MPa, elongation at break of 9.44−9.70% and tensile modulus of 2.09−3.74 GPa. Moreover, the star-branched polyimide films BPI-(1−3) exhibited lower water absorptions of 0.35−0.52%, better dielectric properties with lower dielectric constants of 2.72−3.12 and lower dielectric losses of 0.0028−0.0040 at 1000 kHz.

## 1. Introduction

Over the past few decades, polyimides have attracted more and more attention as one of the most promising high performance polymer materials because of their outstanding comprehensive performance and particularly wide applications in various fields.[1–3] Traditional polyimides, which mainly refers to linear polyimides, possess excellent thermal stability, outstanding mechanical and electrical properties, good chemical resistance, remarkable insulation properties, *etc.*[4,5] Thus they have been widely used in areas like aerospace, microelectronics, coatings, composite materials, and functional membranes.[6–8] With the rapid development of various high-tech fields, the overall performances of polyimides need to meet increasingly complex requirements.[9] As a result, intensive studies have been focused on the preparation of novel linear polyimides and hyperbranched polyimides.

Linear polyimides, aside from the aforementioned advantages, also have some shortcomings. Owing to their rigid backbones and strong intermolecular interactions, most linear polyimides are usually insoluble and infusible which result in

difficult processing and further limit their applications.[10,11] In recent years, tremendous efforts have been invested in developing various melt-processing or organic solvent soluble linear polyimides, which derived from novel diamine or dianhydride having one or more special functional structures, such as flexible linkages,[12–15] bulky substituents,[16–18] fluorinated[19] or sulfur[20] groups, non-coplanar and unsymmetrical structures,[21–23] *etc.* These are effective methods to overcome the above-mentioned shortcomings without sacrificing their inherent excellent thermal and mechanical properties. Due to the low polarizability, small dipole and increased free volume of the C–F bond,[24] fluorinated polyimides possess better optical transparency, solubility as well as lower dielectric constant, water absorption and dissipation factor than traditional polyimides. Therefore, many considerable efforts have been made to the incorporation of fluorinated group into side chain or backbone of the polyimides. Thereupon, novel fluorinated polyimides based on various fluorinated monomers, have been prepared and arouse strong concern for advanced microelectronic and optoelectronic applications.

On the other hand, hyperbranched polyimides as a relatively new class of macromolecules have drawn academia's attentions to the development of novel functional materials. Hyperbranched polyimides are highly branched polymers with unique treelike randomly branching architecture and amounts

*College of Chemistry, Chemical Engineering and Biotechnology, Donghua University, Shanghai 201620, P. R. China. E-mail: wufeng@mail.dhu.edu.cn; yuxinhai@dhu. edu.cn; xpzhou@dhu.edu.cn; Tel: +86 021 67792601*

of terminal groups. Because of the special three-dimensional globular structure, hyperbranched polyimides can provide lower solution viscosity, more excellent solubility and better rheological properties than the traditional linear poly-imides.[25–27] Nowadays hyperbranched polyimides were usually prepared from different types of monomers, mainly including $AB_2$, $A_2 + B_3$, $A_2 + B'B_2$ and $A_2 + B_4$ monomers.[28–31] However, because of the formation of globular macromolecular struc-tures, hyperbranched polymers generally possess poor mechanical properties for the lack of intermolecular entangle-ments, which further severely restrain their applications as the structural materials.[32–34] It is known that the mechanical prop-erties of hyperbranched polyimides are significantly affected by the chain physical entanglements. The incorporation of the increase of the linear moiety and the flexibility of relatively rigid branches into hyperbranched polyimides could be the effective methods to enhance the entanglements of polyimide chains and further improve the mechanical properties of hyper-branched polyimides as Peter J. et al.[33] have demonstrated.

Therefore, in consideration of the advantages and disad-vantages of linear polyimides and hyperbranched polyimides and looking forward to make the best of their advantages and mutually make up their deficiencies, we intend to develop a new class of polymers, star-branched polyimides. In this work, a series of star-branched fluorinated polyimides BPI-(1–3) derived from anhydride-terminated linear poly(amide acid)s LPAA'-(1–3) and a novel fluorinated tetramine, 2,2-bis[4-(2,4-diaminophenoxy)phenyl]hexafluoropropane (BDAPFP), have been successfully synthesized. In comparison, a series of cor-responding linear polyimides LPI-(1–3) were also synthesized by diamine 4,4'-oxybisbenzenamine (ODA), p-phenylenediamine (PDA) and dianhydride 3,3',4,4'-biphenyltetracarboxylic dia-nhydride (BPDA) with various monomer ratios via the two-step procedure with heating imidization method. Direct property comparisons of these polyimides were exhibited, including thermal, optical, mechanical and dielectric properties, water absorption and solubility.

## 2. Experimentation

### 2.1. Materials

Hexafluorobisphenol A, 2,4-dinitrochlorobenzene were purchased from Shanghai EMST Electronic Material Co., Ltd. Anhydrous potassium carbonate ($K_2CO_3$), 85% hydrazine monohydrate ($NH_2NH_2H_2O$) were supplied by Sinopharm Chemical Reagent Beijing Co., Ltd, and used as received. 10% palladium on charcoal (Pd/C) was purchased from Acros. 4,4'-Oxybisbenzenamine (ODA), p-phenylenediamine (PDA) and 3,3',4,4'-biphenyltetracarboxylic di-anhydride (BPDA) were purchased from J&K Chemical Co., Ltd, and the aromatic dia-nhydride BPDA was recrystallized from acetic anhydride and then dried in vacuum at 150 °C for 10 h prior to use. N,N-Dimethylacetamide (DMAc) was purified by vacuum distillation over calcium hydride and stored over 4 Å molecular sieves. All other commercially available reagents and solvents were used without further purification.

### 2.2. Measurements

The FT-IR spectra were recorded on a Thermal Electron Avatar 380 infrared spectrometer at a resolution of 2 cm$^{-1}$ in the range of 400–4000 cm$^{-1}$, with the sample form of powder (monomers) and thin films (polyimides). Nuclear magnetic resonance (NMR) spectra were determined on a Bruker AV 400 MHz spectrometer in DMSO-d$_6$ with tetramethylsilane as internal standard. Chemical shifts ($\delta$) were expressed in ppm. Inherent viscosities ($\eta_{inh}$) of poly(amic acid) (PAA) were measured with an Ubbe-lohde viscometer with 0.5 g dL$^{-1}$ of DMAc solution at 25 °C. The ultraviolet (UV)-visible (Vis) spectra of the films were recorded with a Hitachi U-3310 UV-Vis spectrometer in transmittance mode at room temperature. Dynamic mechanical analysis (DMA) was performed on a Netzsch DMA-242E instrument at a heating rate of 5 °C min$^{-1}$ and a load frequency of 1 Hz in film tension geometry under $N_2$ atmosphere, and the peak temper-ature in the tan $\delta$ curves was regarded as glass transition temperature ($T_g$). Thermo gravimetric analysis (TGA) was con-ducted with the TA instrument TA 2050, with a heating rate of 10 °C min$^{-1}$ in a nitrogen or air flow of 100 ml min$^{-1}$. The mechanical properties of the films were measured by a Zhongzhi CZ-8010 universal testing apparatus at a crosshead speed of 5 mm min$^{-1}$ at room temperature. The size of each film sample was approximately 50 mm × 10 mm × 0.03 mm, and average of at least five individual determinations was used. Dielectric properties of the thin films were studied on a Tonghui Electronics TH2828S Automatic Component Analyzer at room temperature in the frequency range of 10–1000 kHz, the size of each film sample was approximately 15 mm × 15 mm × 0.02 mm. The dielectric constant $\varepsilon$ was then calculated using the equation:

$$\varepsilon = kC_p d / \varepsilon_0 S$$

where $\varepsilon_0$ is the vacuum dielectric constant = $8.85 \times 10^{-12}$ F m$^{-1}$, $C_p$ is the capacitance value of the sample, $S$ is the surface area of the sample = $2.25 \times 10^{-4}$ m$^2$, $d$ is the film thickness, and $k$ is the correction factor of the instrument = 3.15. The capac-itance value and dielectric loss value were directly obtained from the instrument. The water absorption was determined by weighing the change of PI films before and after being immersed in distilled water at room temperature for 24 h.

### 2.3. Synthesis of tetramine monomer

**2.3.1. 2,2-Bis[4-(2,4-dinitrophenoxy)phenyl]hexafluoropropane (BDNPFP).** Hexafluorobisphenol A (3.36 g, 10 mmol), anhydrous potassium carbonate (1.45 g, 10.5 mmol), toluene (85 ml) and N,N-dimethylacetamide (DMAc) (15 ml) were added into a dry three-necked flask equipped with a water separator, a ther-mometer and a reflux condenser. The mixture was heated to refluxing temperature to steam out the generated water and then kept for 2 h with stirring. Next, 2,4-dinitrochlorobenzene (4.15 g, 20.5 mmol) was added into the flask and the mixture was allowed to react at 90 °C for another 5 h. Then the obtained mixture was poured into 200 ml distilled water. The crude product was collected by filtration, washed with hot water, and

dried in vacuum at 100 °C for 10 h. After the crude product was recrystallized from toluene, 6.57 g light yellow solid powder was obtained (yield 98.3%). Melting point: 153.6 °C (the peak temperature of DSC curve). FT-IR (KBr, cm$^{-1}$): 3093 (Ar-H), 1603 (C=C), 1537 (NO$_2$), 1477 (C=C), 1351 (NO$_2$), 1259 (C–N), 1212 (C–O), 1168 (C–F). $^1$H-NMR (400 MHz, DMSO-d$_6$, ppm): 8.94 (d, 1H), 8.52 (m, 1H), 7.54 (d, 2H), 7.42 (m, 2H) and 7.40 (m, 1H), $^{13}$C-NMR (400 MHz, DMSO-d$_6$, ppm): 155.3; 154.2; 142.6; 140.5; 132.6; 130.2; 129.8; 129.3; 128.7; 125.8; 122.9; 122.4; 121.0; 120.5 and 63.9, $^{19}$F-NMR (400 MHz, DMSO-d$_6$, ppm): 63.4 (s, 6F).

**2.3.2. 2,2-Bis[4-(2,4-diaminophenoxy)phenyl]hexafluoropropane (BDAPFP).** Under the protection of nitrogen, 10 g (15 mmol) BDNPFP, 1 g of 10% palladium on activated carbon (Pd/C), 50 ml absolute ethyl alcohol and 30 ml toluene were added into a 250 ml three-necked flask equipped with a dropping funnel, a thermometer and a reflux condenser. The mixture was heated to reflux with stirring, and 20 ml of 85% hydrazine monohydrate was added dropwise in 1 h. After finishing the addition of hydrazine monohydrate, the mixture was refluxed for additional 5 h. Then, the mixture was filtered and the filtrate was concentrated, after cooling in an ice bath, a precipitate separated out, which was collected by filtration, washed with ice ethanol, and dried under vacuum. Finally, 7.14 g white solid powder was obtained (yield 86.8%). Melting point: 200.6 °C (the peak temperature of DSC curve). FT-IR (KBr, cm$^{-1}$): 3420 (NH$_2$), 3316 (NH$_2$), 3212 (Ar-H), 1623 (C=C), 1506 (C=C), 1246 (C–N), 1216 (C–O), 1173 (C–F). $^1$H-NMR (400 MHz, DMSO-d$_6$, ppm): 7.24 (d, 2H), 6.92 (m, 2H), 6.58 (d, 1H), 6.04 (d, 1H), 5.84 (m, 1H), 4.74 (s, 2H) and 4.61 (s, 2H), $^{13}$C-NMR (400 MHz, DMSO-d$_6$, ppm): 159.9; 147.2; 141.4; 131.8; 131.4; 129.4; 128.7; 126.1; 123.2; 125.2; 122.4; 115.8; 103.6; 101.7 and 63.7, $^{19}$F-NMR (400 MHz, DMSO-d$_6$, ppm): 63.4 (s, 6F).

## 2.4. Synthesis of polyimides

The polyimides were synthesized by the conventional two-step procedures *via* poly(amide acid) precursors, followed by thermally curing at elevated temperature. In this study, three star-branched fluorinated polyimides and their corresponding linear polyimides were synthesized.

### 2.4.1. Synthesis of linear polyimides

*2.4.1.1. Synthesis of linear polyimide LPI-1.* Under the protection of nitrogen, diamine ODA (2.0024 g 10 mmol), dianhydride BPDA (2.9422 g 10 mmol) and freshly distilled DMAc

(38 ml) were added into a dry three-neck flask. The reaction mixture was kept stirring at room temperature for 12 h to yield a yellow viscous poly(amide acid) (PAA) solution LPAA-1. Then, the LPI-1 film was prepared *via* a PAA solution casting method. The LPAA-1 solution was cast onto dust-free glass plates and then thermally cured in an oven for 1 h at each of 100, 200 and 300 °C. Finally, the LPI-1 film was obtained by immersing the glass plates in warm water and drying at 100 °C for 2 h. The synthesis route was shown in Scheme 2.

FT-IR: 1773, 1719 cm$^{-1}$ (C=O asymmetrical and symmetrical stretching, imide), 1374 cm$^{-1}$ (C–N stretching, imide), 735 cm$^{-1}$ (imide ring deformation).

*2.4.1.2. Synthesis of linear polyimide LPI-2.* Under the protection of nitrogen, diamine PDA (1.0814 g 10 mmol), dianhydride BPDA (2.9422 g 10 mmol) and freshly distilled DMAc (31 ml) were added into a dry three-neck flask, and the procedures that followed were the same as in the preparation of the linear polyimide LPI-1.
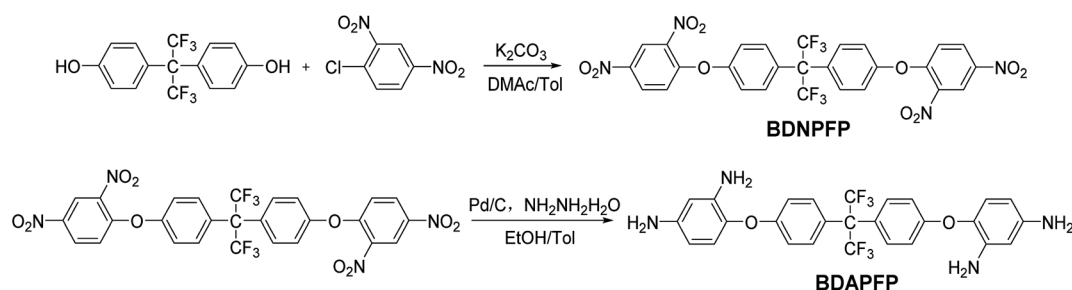
FT-IR: 1774, 1722 cm$^{-1}$ (C=O asymmetrical and symmetrical stretching, imide), 1359 cm$^{-1}$ (C–N stretching, imide), 736 cm$^{-1}$ (imide ring deformation).

*2.4.1.3. Synthesis of linear copolyimide LPI-3.* Under the protection of nitrogen, diamine PDA (0.5407 g 5 mmol) and ODA (1.0012 g 5 mmol), dianhydride BPDA (2.9422 g 10 mmol) and freshly distilled DMAc (33 ml) were added into a dry three-neck flask, and the procedures that followed were the same as in the preparation of the linear polyimide LPI-1.

FT-IR: 1774, 1722 cm$^{-1}$ (C=O asymmetrical and symmetrical stretching, imide), 1366 cm$^{-1}$ (C–N stretching, imide), 737 cm$^{-1}$ (imide ring deformation).

### 2.4.2. Synthesis of star-branched polyimides.

The star-branched polyimides derived from their corresponding anhydride-terminated linear poly(amide acid) LPAA'-(1–3) and the fluorinated tetramine monomer BDAPFP synthesized above.

*2.4.2.1. Synthesis of star-branched polyimide BPI-1.* Under the protection of nitrogen, diamine ODA (2.0024 g 10 mmol), dianhydride BPDA (3.8249 g 13 mmol) and freshly distilled DMAc (43 ml) were added into a dry three-neck flask. The reaction mixture was kept stirring at room temperature for 6 h to yield a yellow viscous anhydride-terminated linear poly(amide acid) solution LPAA'-1. Then, the tetramine monomer BDAPFP (0.4114 g 0.75 mmol) was added to the mixture. After 6 h stirring at room temperature, a viscous tawny star-branched poly(amide acid) solution BPAA-1 was obtained. After that, the BPI-1 film was also prepared *via*



**Scheme 1** Synthesis route of tetramine monomer.
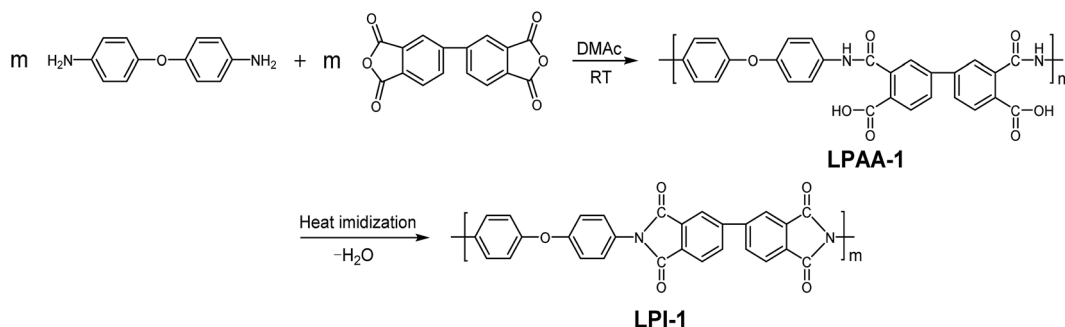
**Scheme 2** Synthesis route of linear polyimide LPI-1.

a PAA solution casting method. The BPAA-1 solution was cast onto clean glass plates and then thermally cured in an oven for 1 h at each of 100, 200 and 300 °C. Finally, the BPI-1 film was obtained by immersing the glass plates in warm water and drying at 100 °C for 2 h. The synthesis route was shown in Scheme 3.

FT-IR: 1848 cm$^{-1}$ (C=O stretching, terminal anhydride), 1774, 1720 cm$^{-1}$ (C=O asymmetrical and symmetrical stretching, imide), 1376 cm$^{-1}$ (C–N stretching, imide), 737 cm$^{-1}$ (imide ring deformation).

*2.4.2.2. Synthesis of star-branched polyimide BPI-2.* Under the protection of nitrogen, diamine PDA (1.0814 g 10 mmol), dianhydride BPDA (3.8249 g 13 mmol) and freshly distilled DMAc (36 ml) were added into a dry three-neck flask, and the procedures that followed were the same as in the preparation of the star-branched polyimide BPI-1.

FT-IR: 1847 cm$^{-1}$ (C=O stretching, terminal anhydride), 1774, 1721 cm$^{-1}$ (C=O asymmetrical and symmetrical stretching, imide), 1359 cm$^{-1}$ (C–N stretching, imide), 736 cm$^{-1}$ (imide ring deformation).

*2.4.2.3. Synthesis of star-branched copolyimide BPI-3.* Under the protection of nitrogen, diamine PDA (0.5407 g 5 mmol) and ODA (1.0012 g 5 mmol), dianhydride BPDA (3.8249 g 13 mmol) and freshly distilled DMAc (39 ml) were added into a dry three-

neck flask, and the procedures that followed were the same as in the preparation of the star-branched polyimide BPI-1.

FT-IR: 1845 cm$^{-1}$ (C=O stretching, terminal anhydride), 1774, 1721 cm$^{-1}$ (C=O asymmetrical and symmetrical stretching, imide), 1364 cm$^{-1}$ (C–N stretching, imide), 736 cm$^{-1}$ (imide ring deformation).

## 3. Results and discussion

### 3.1. Monomer synthesis

A novel aromatic tetramine BDAPFP was synthesized *via* a two-step procedures as shown in Scheme 1. First, the intermediate tetranitro compound BDNPFP was prepared by a nucleophilic chlorine-displacement reaction of 2,4-dinitrochlorobenzene with hexafluorobisphenol A in the presence of anhydrous potassium carbonate in toluene and DMAc. The *para* and *ortho* nitro group activated the chlorine atom for displacement, therefore, the chlorine-displacement reaction of 2,4-dinitro-chlorobenzene by the phenoxide anion was readily carried out.[24] Second, the fluorinated tetramine monomer BDAPFP was synthesized in high yield by the hydrazine reduction reaction of BDNPFP catalyzed with Pd/C in ethyl alcohol and toluene at refluxing temperature for several hours.
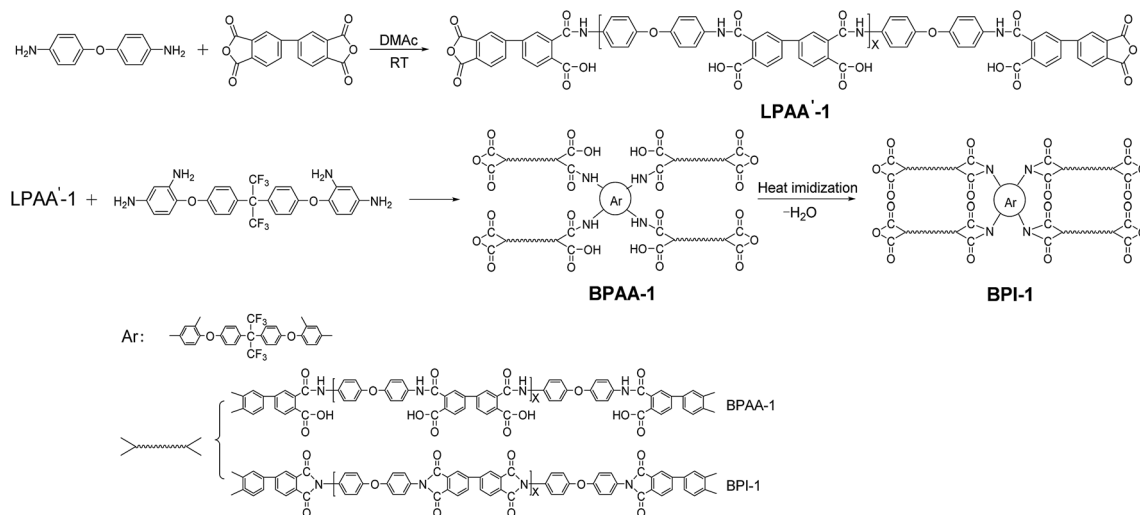


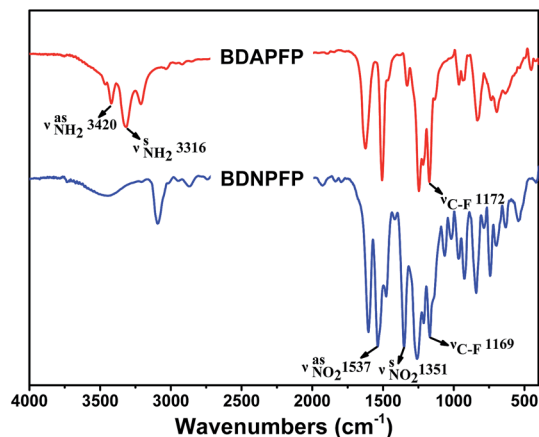**Scheme 3** Synthesis route of star-branched polyimide BPI-1.

Fig. 1   FT-IR spectra of BDNPFP and BDAPFP (KBr sample).

The chemical structures of BDNPFP and BDAPFP were characterized by FT-IR, $^1$H-NMR, $^{13}$C-NMR and $^{19}$F-NMR. Fig. 1 shows the FT-IR spectra of tetranitro compound BDNPFP and tetramine monomer BDAPFP. The nitro groups of BDNPFP gave two characteristic peaks at 1537 and 1351 cm$^{-1}$ (NO$_2$ asymmetric and symmetric stretching). After the reduction, the characteristic absorptions of the nitro groups disappeared, and the amino groups showed a pair of N–H stretching bands at 3420 and 3316 cm$^{-1}$ (NH$_2$ asymmetric and symmetric stretching). As shown in Fig. 2, $^1$H-NMR spectrum of the tetramine BDAPFP illustrated that the nitro groups in BDNPFP were completely reduced, in which the signals of amino groups appeared at around $\delta$ 4.74 (*para* amino) and 4.61 (*ortho* amino) as two singlets, signals at $\delta$ 7.24, 6.92, 6.58, 6.04 and 5.84 derived from the benzene rings. In $^{13}$C-NMR spectra, the total 27 carbon atoms in BDAPFP showed 15 signals, which resonated in the region of 63.7–159.9 ppm. Owing to the coupling effect of the strong electrophilic fluorine atoms, the signals of carbon atom C$^{12}$ in trifluoromethyl group split up into four singlets ($\delta$ 129.4, 128.7, 126.1 and 123.2). The carbon atom C$^{11}$ showed a singlet at around $\delta$ 63.7. In $^{19}$F-NMR spectra, the six fluorine atoms in BDAPFP only appeared a singlet at around $\delta$ 63.4. All of the above results confirm the chemical structure of the tetramine monomer BDAPFP.

## 3.2.   Polymer synthesis

Two commercially available aromatic diamine ODA and PDA were reacted with one aromatic dianhydride BPDA with various monomer ratios to give three linear polyimides LPI-(1–3), and three corresponding star-branched polyimides BPI-(1–3) were synthesized by the anhydride-terminated linear poly(amide acid)s LPAA'-(1–3) and the obtained tetramine monomer BDAPFP. The new polyimides were synthesized by the two-step method, which were carried out *via* poly(amide acid)s intermediate. The polymerization of linear polyimide was carried out by reacting equimolar amounts of diamine monomer with aromatic dianhydride at a concentration of 12% solids in DMAc. In the polymerization of star-branched polyimide, excess aromatic dianhydride reacted with diamine monomer to form
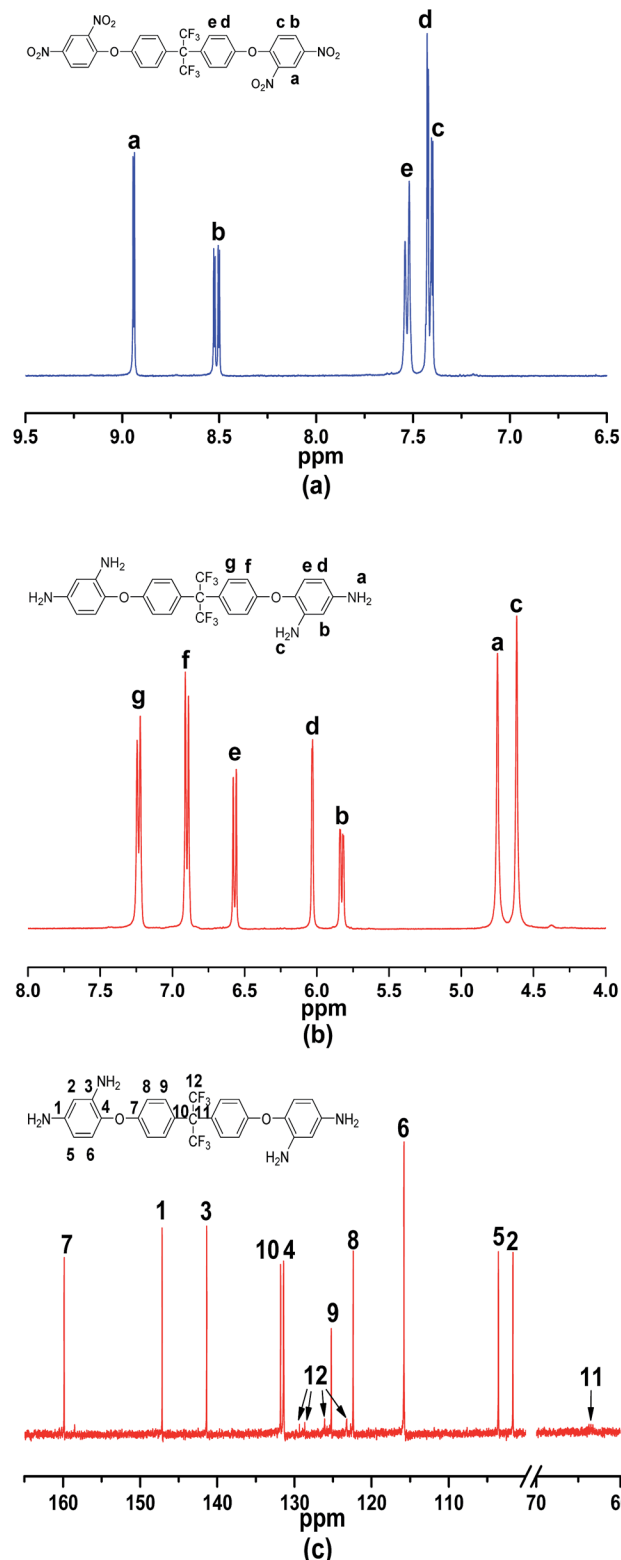


Fig. 2   $^1$H-NMR (a) spectra of BDNPFP and $^1$H-NMR (b) and $^{13}$C-NMR (c) spectra of BDAPFP.

the anhydride-terminated linear poly(amide acid), then the tetramine monomer BDAPFP as branching point reacted with the obtained anhydride-terminated linear poly(amide acid) to

**Table 1** Inherent viscosity of the PAA and thermal properties of the polyimides

| Polyimides | $\eta_{inh}{}^a$ of PAA (dL g$^{-1}$) | $T_g{}^b$ (°C) | $T_{5\%}{}^c$ (°C) | | $T_{10\%}{}^c$ (°C) | | $R_{w800}{}^d$ (%) |
|---|---|---|---|---|---|---|---|
| | | | N$_2$ | Air | N$_2$ | Air | |
| LPI-1 | 1.88 | 272.4 | 539 | 495 | 564 | 535 | 56.6 |
| BPI-1 | 1.92 | 283.0 | 544 | 500 | 571 | 537 | 59.4 |
| LPI-2 | 2.26 | 313.3 | 559 | 534 | 586 | 574 | 55.7 |
| BPI-2 | 2.32 | 318.0 | 578 | 560 | 599 | 595 | 58.6 |
| LPI-3 | 2.09 | 285.1 | 551 | 542 | 577 | 572 | 57.2 |
| BPI-3 | 2.14 | 289.7 | 569 | 547 | 588 | 579 | 59.2 |

$^a$ $\eta_{inh}$: inherent viscosity, measured at 25 °C at polymer concentration of 0.5 dL g$^{-1}$ in DMAc. $^b$ $T_g$: glass transition temperature, obtained at the peak temperature in the tan δ curves, with a heating rate of 5 °C min$^{-1}$ and a load frequency of 1 Hz in film tension geometry under N$_2$ atmosphere. $^c$ $T_{5\%}$, $T_{10\%}$: temperatures at 5% and 10% weight loss measured by TGA at a heating rate of 10 °C min$^{-1}$, respectively. $^d$ $R_{w800}$: residual weight ratio at 800 °C by TGA at a heating rate of 10 °C min$^{-1}$ in nitrogen.

get a star-branched poly(amide acid) at a 12% solid content. The polycondensation reaction was conducted at room temperature for 12–16 h to yield PAA solution. As shown in Table 1, the inherent viscosities of the PAA precursors were 1.88–2.32 dL g$^{-1}$, indicating that the polymers with relatively high molecular weights were obtained. Tough and flexible polyimide films were obtained by casting the PAA solution on the glass plate followed by thermally curing process at 300 °C. It is intriguing to observe that the inherent viscosities of the synthesized star-branched polyimides were relatively higher than that of corresponding linear polyimides, which gives rise to a little confusion about the common knowledge that the hyperbranched polymers are usually thought to be low in inherent viscosity. However, the reason for the phenomenon is unclear yet.[34,35]

The structures of polyimides were confirmed by FT-IR, as shown in Fig. 3. The absence of the characteristic peaks of poly(amide acid) around 1660 cm$^{-1}$ and the appearance of the characteristic peaks of the imide ring around 1774 cm$^{-1}$, 1720 cm$^{-1}$, 1359–1376 cm$^{-1}$ and 736 cm$^{-1}$ in FTIR spectra suggest a complete conversion of poly(amide acid) into the polyimide. The strong absorption bands were observed in the region of 1100–1300 cm$^{-1}$ due to the C–O–C and C–F multiple stretching. In addition, the band around 1847 cm$^{-1}$ attributed to the

stretching of C=O of the terminal anhydride group[36,37] was found in the spectrum of the star-branched polyimides, indicating that the synthesized star-branched polyimides were all anhydride-terminated. Besides, the spectrum of the star-branched polyimides did not show any absorption in the range of 3100–3450 cm$^{-1}$, demonstrating that the tetramine monomer BDAPFP was completely consumed and transformed into the branch points of the star-branched polyimides.

### 3.3. Thermal properties

The thermal properties of the polyimides BPI-(1–3) and LPI-(1–3) were evaluated by dynamic mechanical analysis (DMA) and thermo gravimetric analysis (TGA). The results are summarized in Table 1. Glass transition temperatures ($T_g$) of the polyimides were in the range of 272.4–318.0 °C, as shown in Fig. 4. Generally, $T_g$ values of polymers are determined by molecular packing and chain rigidity of the polymer backbones. As a result, $T_g$ values of the linear polyimides followed an order of LPI-2 > LPI-3 > LPI-1, which might be due to the decrease in chain rigidity with the existence of more ether groups. Moreover, the $T_g$ values of the star-branched polyimides BPI-(1–3) were a little higher than the relevant data of corresponding linear polyimides LPI-(1–3), which could be attributed to the
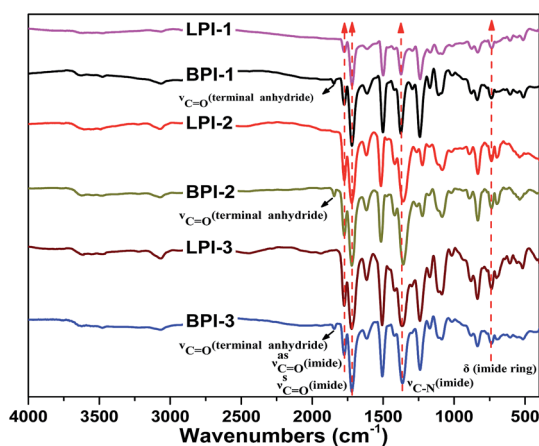


**Fig. 3** FT-IR spectra of the polyimide films.
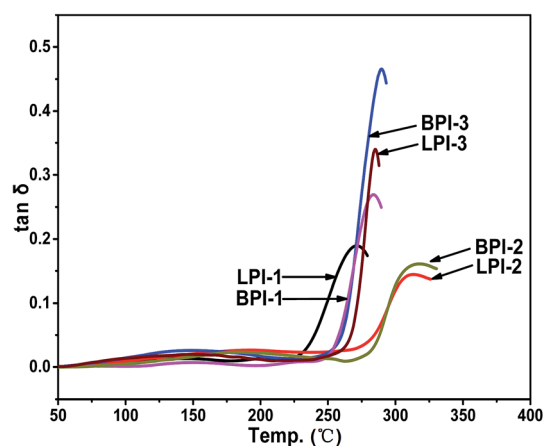


**Fig. 4** Loss tangent of the polyimides.

more rigid molecular chain structure that resulted from the introduction of the tetramine BDAPFP as the crosslinking.

The thermal stabilities of the polyimides were evaluated by TGA in both nitrogen and air atmosphere as shown in Fig. 5, and the results were summarized in Table 1. The decomposition temperatures at 5% weight loss of the polyimides in nitrogen and air were recorded in the range of 539–578 °C and 495–560 °C, respectively. Furthermore, the residual weight retentions at 800 °C were in the range of 55.7–59.4%. The TGA results indicated that the synthesized polyimides had fairly high thermal stability. There was only one stage in the process of thermal decomposition according to the TGA curves, and the decomposition of main chains occurred during this stage. The 5% and 10% weight loss temperatures in nitrogen and air and the residue weight rate at 800 °C in nitrogen of star-branched polyimides BPI-(1–3) were all higher than the corresponding linear polyimides LPI-(1–3). It suggested that the star-branched polyimides derived from the tetramine BDAPFP possessed excellent thermal stability, which might be ascribed to the branched three-dimensional

network structures. In addition, the LPI-1 showed the worst thermal stability among all the three linear polyimides LPI-(1–3), implying the easy degradation in the heating process for the presence of largest amount of flexible ether linkage in the diamine moiety, while the LPI-2 exhibited better thermal stability for the wholly aromatic molecular chain structure compared with other linear polyimides.

### 3.4. Optical properties

To estimate the optical transparency of the polyimide films, the UV-Vis absorption spectra of the polyimides with thicknesses of approximately 10 μm were shown in Fig. 6, and the corresponding cut-off wavelength (absorption edge, $\lambda_{cutoff}$) values and transmittance at 800 nm were listed in Table 2. We can find that all the polyimides exhibited good optical transparency with $\lambda_{cutoff}$ of 366–398 nm and transmittances of 76–86% at 800 nm. All three star-branched polyimides BPI-(1–3) showed a little higher transmittance and a slightly lower cut-off wavelength than the corresponding linear polyimides LPI-(1–3). These results might be attributed to the reduction of the intermolecular charge-transfer complex (CTC) under the influence of the tetramine BDAPFP as the crosslinking. As reported by S. Ando,[38] the bulky and electron-withdrawing $CF_3$ groups in the tetramine BDAPFP could significantly inhibit the CTC formation between polymer chains through steric hindrance and the inductive effect (by decreasing the electron-donating property of the tetramine moieties). Moreover, the $CF_3$ groups might weaken chain-to-chain cohesive force due to lower polarizability of the C–F bond. It can be observed from Fig. 6 that the LPI-1 derived only from BPDA and ODA containing the most ether linkages in the polymer backbone exhibited the shortest $\lambda_{cutoff}$ and the highest transparency at 800 nm among all the three linear polyimides LPI-(1–3). This phenomenon was due to the fact that the ether linkages could lead to the reduction of the intermolecular CTC formation.

### 3.5. Mechanical properties

In this study, the star-branched polyimides derived from the anhydride-terminated linear poly(amide acid) and the
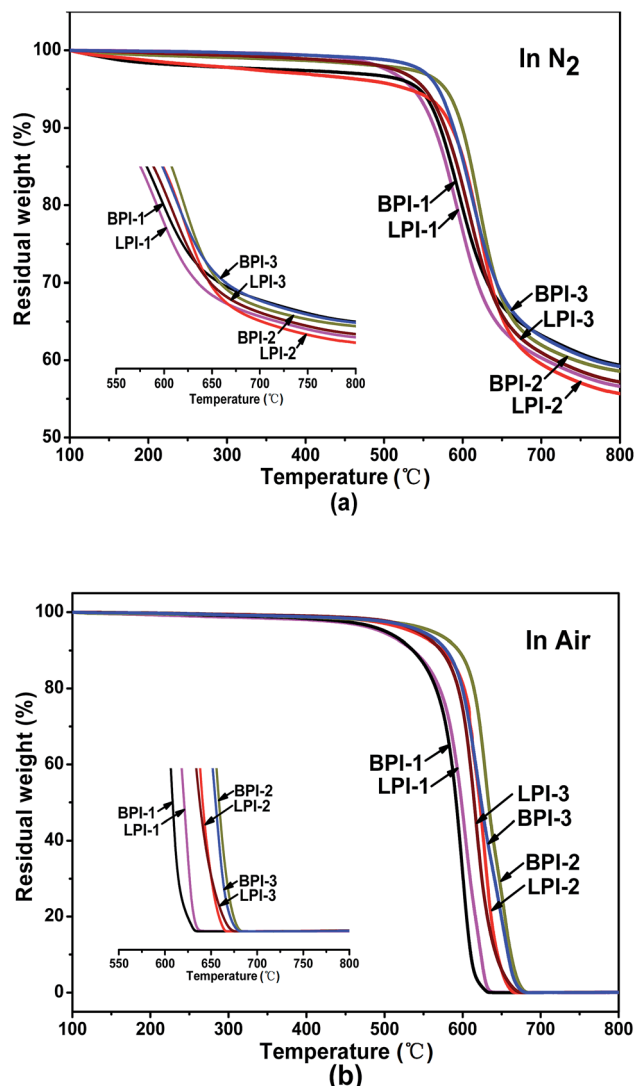


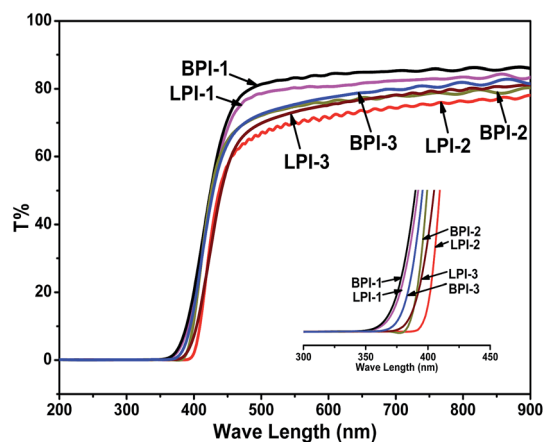Fig. 5 TGA curves of the polyimides ((a) in $N_2$, (b) in air).



Fig. 6 UV–visible spectra of the PI films.

This journal is © The Royal Society of Chemistry 2017

Table 2  Optical and mechanical properties of the polyimides

| Polyimides | $T_{800}^a$ (%) | $\lambda_{cutoff}^b$ (nm) | $T_S^c$ (MPa) | $T_M^d$ (GPa) | $E_B^e$ (%) |
|---|---|---|---|---|---|
| LPI-1 | 84 | 370 | 101 | 1.92 | 9.70 |
| BPI-1 | 86 | 366 | 113 | 2.09 | 9.03 |
| LPI-2 | 76 | 398 | 218 | 3.44 | 9.44 |
| BPI-2 | 79 | 388 | 243 | 3.74 | 8.50 |
| LPI-3 | 80 | 386 | 137 | 2.54 | 9.68 |
| BPI-3 | 82 | 378 | 150 | 2.80 | 8.87 |

[a] $T_{800}$: transmittance at 800 nm. [b] $\lambda_{cutoff}$: cut off wavelength. [c] $T_S$: tensile strength. [d] $T_M$: tensile modulus. [e] $E_B$: elongation at break.

tetramine monomer BDAPFP were intentionally designed to improve the mechanical property. As anticipated, the star-branched polyimides exhibited favorable mechanical properties with tensile strength of 113–243 MPa, elongations at break of 9.44–9.70% and tensile modulus of 2.09–3.74 GPa as listed in Table 2. Moreover, all the star-branched polyimides BPI-(1–3) showed the obviously higher tensile strength and tensile modulus and lower elongations at break than the corresponding linear polyimides LPI-(1–3), which can be attributed to the more rigid branching chain structure. The mechanical properties of the linear polyimides followed an order of LPI-2 > LPI-3 > LPI-1. It might be due to the decrease in chain rigidity with increasing the ether groups. These results indicated that the synthesized polyimide films were strong and tough polymer materials.

## 3.6.  Dielectric properties and water absorption

The dielectric constant, dielectric loss and water absorption of the polyimides are shown in Table 3. The dielectric constants of all the polyimides were located in the range of 2.72–3.39 at 1000 kHz, which were lower than the commercial Kapton film (3.67 at 1000 kHz).[39] And the star-branched polyimides (BPI-(1–3)) showed lower dielectric constant than the corresponding linear polyimides (LPI-(1–3)) in the frequency range of 10–1000 kHz. This result was caused by the existence of the pendant CF$_3$ groups in the tetramine structure, which prevent the chain packing and increased the free volume. As shown in the results, the star-branched polyimides BPI-(1–3) also exhibited lower dielectric loss than the corresponding linear polyimides LPI-(1–3), resulting from the more symmetric molecular chain

structure after branching, which led to a decline in polarity, and then decreased the dielectric loss. For each polyimide, with increasing the frequency from 10 to 1000 kHz, the dielectric constant decreased and the dielectric loss increased. These variations were attributed to the frequency dependence of the polarization mechanisms, which comprise the dielectric constant and dielectric loss.

The water absorption of the polyimides also has a significant influence on the dielectric properties in microelectronic field, and polyimide with low water absorption possesses stable dielectric properties. As shown in Table 3, the water absorption values were in the range of 0.35–1.07%, which were obtained by testing at least three parallel samples. All the synthesized star-branched polyimides BPI-(1–3) presented lower water absorption than the corresponding linear polyimides LPI-(1–3). It might be attributed to the presence of –CF$_3$ functional groups in polyimide backbone which possess hydrophobic features and inhibit the absorption of moisture molecules on the polymer surfaces.

## 3.7.  Solubility

The solubility of the polyimide films was determined at 10 mg ml$^{-1}$ (polymer/solvent) at room temperature for 24 h in various organic solvents. All the star-branched polyimide films BPI-(1–3) and the linear polyimide films LPI-(1–3) exhibited poor solubility in strong polar solvents, such as N,N-dimethylaceta-mide, N,N-dimethylformamide and N-methyl-2-pyrrolidone, which might result from the crosslinking structure generated among imide ring and aromatic ring at the elevated temperature.[31,40] These results indicated that the star-branched poly-imide did not effectively improve the solubility of the film compared with linear polyimide. In theory, the star-branched polyimide possesses lower chain packing density and weaker intermolecular interaction which are favorable factors for solubility improvement. However, it is still insufficient to enhance the solubility of the film in the experiment. What's more, the diamine PDA, ODA and dianhydride BPDA we chose in this study are wholly aromatic short-chain compounds with strong rigid groups such as benzene ring and biphenyl group. It is very easy to generate particularly high chain packing density and unfavorable strong intermolecular interaction when react to form the linear moiety of the polyimide, so the compact molecular chain structures of the linear polyimides and the

Table 3  Dielectric properties and water absorption of the polyimides

| Polyimides | tan $\delta^a$ | | | $\varepsilon^b$ | | | $w^c$ (%) |
|---|---|---|---|---|---|---|---|
| | 10 kHz | 100 kHz | 1000 kHz | 10 kHz | 100 kHz | 1000 kHz | |
| LPI-1 | 0.0031 | 0.0039 | 0.0044 | 3.43 | 3.40 | 3.39 | 1.07 |
| BPI-1 | 0.0024 | 0.0030 | 0.0040 | 3.16 | 3.15 | 3.12 | 0.52 |
| LPI-2 | 0.0022 | 0.0028 | 0.0034 | 3.09 | 3.08 | 3.07 | 0.99 |
| BPI-2 | 0.0020 | 0.0024 | 0.0028 | 2.74 | 2.73 | 2.72 | 0.35 |
| LPI-3 | 0.0024 | 0.0030 | 0.0036 | 3.16 | 3.15 | 3.12 | 1.03 |
| BPI-3 | 0.0022 | 0.0026 | 0.0029 | 2.86 | 2.84 | 2.83 | 0.47 |

[a] tan $\delta$: dielectric loss. [b] $\varepsilon$: dielectric constant. [c] $w$: water absorption.

star-branched polyimides are too rigid to dissolve. Therefore, selecting diamine and dianhydride with more functional groups such as flexible groups, long-chain alkyl groups and bulky lateral pendants that can reduce the rigidity of the molecular skeleton would be an effective way to prepare the soluble star-branched polyimide. We are going to run the follow up experiments to further improve the solubility and possibly publish the results in the future.

## 4. Conclusions

A novel aromatic fluorinated tetramine was synthesized and characterized, which was employed to react with various anhydride-terminated linear poly(amide acid)s to yield a series of fluorinated star-branched polyimides *via* the two-step polymerization method. The resulting star-branched polyimides presented more excellent thermal stability, more outstanding mechanical properties, better optical and dielectric properties, lower water absorption than the linear polyimides. Thus, the star-branched polyimides might have potential applications in microelectronic, photoelectric and optical fields.

## Acknowledgements

## References

1 C. Sroog, *History of the invention and development of the polyimides*, Marcel Dekker, Inc, New York, 1996.

2 K. L. Mittal, *Polyimides: synthesis, characterization, and applications*, Springer Science & Business Media, 2013.

3 D. Liaw, K. Wang, Y. Huang, K. Lee, J. Lai and C. Ha, *Prog. Polym. Sci.*, 2012, **37**, 907–974.

4 M. Ghosh, *Polyimides: fundamentals and applications*, CRC Press, 1996.

5 Q. Gong, S. Gong, H. Zhang, L. Liu and Y. Wang, *RSC Adv.*, 2015, **5**, 57245–57253.

6 X. Ma, R. Swaidan, Y. Belmabkhout, Y. Zhu, E. Litwiller, M. Jouiad, I. Pinnau and Y. Han, *Macromolecules*, 2012, **45**, 3841–3849.

7 L. Y. Jiang, Y. Wang, T. S. Chung, X. Y. Qiao and J. Y. Lai, *Prog. Polym. Sci.*, 2009, **34**, 1135–1160.

8 A. K. Naskar and D. D. Edie, *J. Compos. Mater.*, 2006, **40**, 1871–1883.

9 Y. Guan, C. Wang, D. Wang, G. Dang, C. Chen, H. Zhou and X. Zhao, *Polymer*, 2015, **62**, 1–10.

10 H. Behniafar and P. Boland, *J. Polym. Res.*, 2010, **17**, 511–518.

11 X. Yu, D. I. Machanje, B. Xu and Y. Xu, *J. Macromol. Sci., Part B: Phys.*, 2013, **52**, 489–503.

12 Z. Qiu, J. Wang, Q. Zhang, S. Zhang, M. Ding and L. Gao, *Polymer*, 2006, **47**, 8444–8452.

13 D. S. Reddy, C. Chou, C. Shu and G. Lee, *Polymer*, 2003, **44**, 557–563.

14 X. Huang, W. Huang, Y. Zhou and D. Yan, *Chin. J. Polym. Sci.*, 2011, **29**, 506–512.

15 J. J. Zhao, C. L. Gong, S. J. Zhang, Y. Shao and Y. F. Li, *Chin. Chem. Lett.*, 2010, **21**, 277–278.

16 Y. Liu, Y. Xing, Y. Zhang, S. Guan, H. Zhang, Y. Wang, Y. Wang and Z. Jiang, *J. Polym. Sci., Part A: Polym. Chem.*, 2010, **48**, 3281–3289.

17 C. H. Lin, S. L. Chang and P. W. Cheng, *Polymer*, 2011, **52**, 1249–1255.

18 L. Yi, W. Huang and D. Yan, *J. Polym. Sci., Part A: Polym. Chem.*, 2017, **55**, 533–559.

19 L. Yi, C. Li, W. Huang and D. Yan, *J. Polym. Sci., Part A: Polym. Chem.*, 2016, **54**, 976–984.

20 N. You, Y. Suzuki, D. Yorifuji, S. Ando and M. Ueda, *Macromolecules*, 2008, **41**, 6361–6366.

21 M. Taghavi, M. Ghaemy, M. Hassanzadeh and S. M. A. Nasab, *Chin. J. Polym. Sci.*, 2013, **31**, 679–690.

22 P. Thiruvasagam, *Des. Monomers Polym.*, 2014, **17**, 166–175.

23 C. Wang, X. Zhao and G. Li, *Chin. J. Chem.*, 2012, **30**, 2466–2472.

24 Y. Guan, D. Wang, G. Song, G. Dang, C. Chen, H. Zhou and X. Zhao, *Polymer*, 2014, **55**, 3634–3641.

25 Y. Song, H. Yao, Y. Lv, S. Zhu, S. Liu and S. Guan, *RSC Adv.*, 2016, **6**, 93094–93102.

26 X. Lei, M. Qiao, L. Tian, Y. Chen and Q. Zhang, *J. Phys. Chem. C*, 2016, **120**, 2548–2561.

27 J. M. Fréchet, C. J. Hawker, I. Gitsov and J. W. Leon, *J. Macromol. Sci., Part A: Pure Appl. Chem.*, 1996, **33**, 1399–1425.

28 K. L. Wang, M. Jikei and M. a. Kakimoto, *J. Polym. Sci., Part A: Polym. Chem.*, 2004, **42**, 3200–3211.

29 J. Hao, M. Jikei and M. a. Kakimoto, *Macromolecules*, 2003, **36**, 3519–3528.

30 D. H. Bolton and K. L. Wooley, *J. Polym. Sci., Part A: Polym. Chem.*, 2002, **40**, 823–835.

31 S. Liu, S. Zhu, X. Wang, H. Tan and S. Guan, *High Perform. Polym.*, 2016, 1–12.

32 Y. Zheng, S. Li, Z. Weng and C. Gao, *Chem. Soc. Rev.*, 2015, **44**, 4091–4130.

33 J. Peter, A. Khalyavina, J. Kriz and M. Bleha, *Eur. Polym. J.*, 2009, **45**, 1716–1727.

34 S. Liu, Y. Zhang, X. Wang, H. Tan, N. Song and S. Guan, *RSC Adv.*, 2015, **5**, 107793–107803.

35 J. Hao, M. Jikei and M. a. Kakimoto, *Macromolecules*, 2002, **35**, 5372–5381.

36 J. Fang, H. Kita and K. i. Okamoto, *Macromolecules*, 2000, **33**, 4639–4646.

37 H. Chen and J. Yin, *J. Polym. Sci., Part A: Polym. Chem.*, 2002, **40**, 3804–3814.

38 S. Ando, T. Matsuura and S. Sasaki, *Polym. J.*, 1997, **29**, 69–76.

39 C. P. Yang, R. S. Chen and K. H. Chen, *J. Polym. Sci., Part A: Polym. Chem.*, 2003, **41**, 922–938.

40 M. I. Bessonov and V. A. Zubkov, *Polyamic acids and polyimides: synthesis, transformations, and structure*, CRC Press, 1993.